Freeform Shading and Lighting Systems from Planar Quads

Caigui Jiang[1]
Jun Wang [1]
Philippe Bompas [2]
Helmut Pottmann [3]
Johannes Wallner [1,4]

The topic of this paper is optimized shading and lighting systems which consist of planar fins arranged along the edges of a quad-dominant base mesh, that mesh itself covering a reference surface. Such an arrangement can be observed e.g. in the *Kogod courtyard* roof designed by Foster + Partners for the National Portrait Gallery in Washington DC (Fig. 1): A reference surface consisting of three vaults with curved valleys in between is panelized by a quad mesh whose faces are not planar; planar glass panels are mounted on a grid of quadrilateral fins which follow the edges of the quad mesh. In our paper we consider structures of exactly that type, whose geometry is hierarchically set up as follows:

- The first element in the hierarchy is the reference surface, which may be any freeform shape.
- Secondly, the reference surface is panelized by a quad-dominant mesh, which is referred to as the *base mesh*.
- Thirdly, *planar fins* are arranged along the edges of the base mesh such that in each vertex the planes of fins nicely intersect in a common *node axis*.

For the purposes of this paper, the primary hierarchy – the reference shape – is given, while the second and third hierarchies are to be determined by geometric objectives like maximal shading or the guiding of light by reflection. It turns out that these second and third levels (mesh and fins) are intimately connected to each other and cannot be chosen individually and independently. The total of all three levels together is called a *torsion-free support structure*.

It is an important point we wish to make that even in case the primary surface is flat (like an ordinary vertical facade, or a flat roof), the secondary and tertiary level are still freeform.

Here we briefly review the geometric background, demonstrate results of geometry optimization, and discuss its application to the design of reflection patterns. We continue with manufacturing issues, and we conclude with the stability and rigidity/flexibility of support structures.

Figure 1: Kogod Courtyard, Smithsonian National Portrait Gallery, Washington DC. The glass canopy, designed by Foster + Partners, represents an arrangement of quadrilaterals which follow the edges of a quad mesh and which actually constitute a torsion-free support structure.

[1] King Abdullah University of Science and Technology, Thuwal 23955, Saudi Arabia
[2] Architect, 170 rue du Temple, 75003 Paris, France
[3] Graz University of Technology, 8010 Graz, Austria
[4] Vienna University of Technology, 1040 Wien, Austria

PREVIOUS WORK AND GEOMETRIC BASICS OF TORSION-FREE SUPPORT STRUCTURES

From the abstract viewpoint of geometry, our objects of study are quad-dominant meshes with additional decoration: each vertex (resp., node) is equipped with a node axis, and each edge is equipped with a plane carrying the fins. In order to represent a torsion-free support structure, these two items must be consistent: If an edge contains a node, its corresponding plane contains the node axis (see Fig. 1, center). The faces of the base mesh (realized as glass panels in Fig. 1, right) are of no concern in this paper.

(Wang et al., 2013) propose a computational approach for the modeling and optimization of such support structures which satisfy constraints like the blocking of light, and which comply with designers' wishes like boundary alignment or prescribed lines of sight. This modeling procedure entails two steps, which we do not present in detail here. The first is to optimize a field of node axes for a dense sample of vertices placed on the reference surface (without knowing the final location of nodes and edges yet). It turns out that indeed it is best from the computational viewpoint to have the node axes as variables in optimization. A result of that optimization procedure can be seen in Fig. 2a. In a second step one extracts a quad mesh such that the previously obtained axes are usable for a support structure with planar fins (one has to choose edges such that the node axes at either end are co-planar). The second step is conceptually very similar to finding a mesh whose edges follow the principal directions of curvature, see Fig. 2a and Fig. 2b. Finally one has to apply global optimization to ensure planarity of fins, see Fig. 2c.

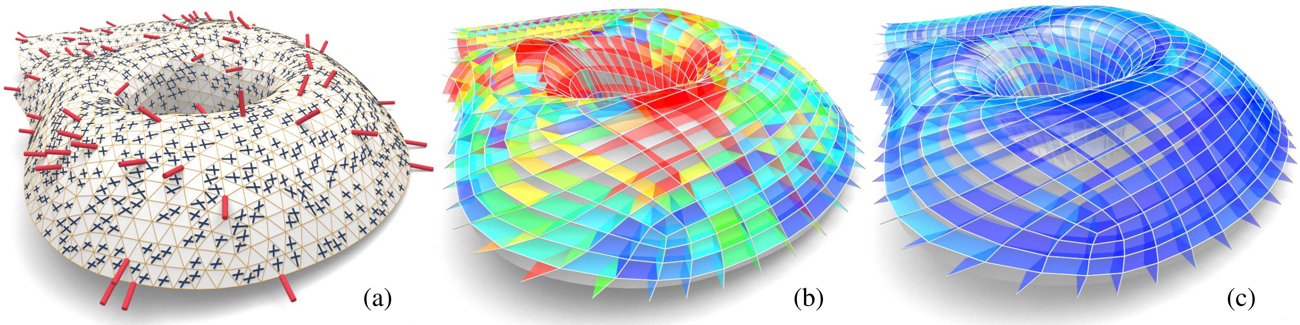

Figure 2: Typical example of optimization procedure, after node axes have already been determined for a dense sample of points on the reference surface. (a) shows a small selection of node axes (red) and also a sample of the "principal" directions (blue) which correspond to this system of node axes. They are determined by methods of differential geometry, cf. (Pottmann and Wallner, 2001). (b) already shows the 2nd and 3rd geometry layers which augment the reference surface: A quad mesh whose edges follow the principal directions, and quadrilateral fins which are spanned by the edges and node axes. The quads which occur here are already approximately planar, so the arrangement of quads is already close to a support structure. Subfigure (c) shows the support structure after global optimization such that fins become planar. The degree of planarity is shown by color coding: the red color corresponds to quads which are off a plane by 2% of their diameter. These figures are taken from (Wang et al., 2013).

The present paper is not concerned with details of those methods of optimization, which would anyway fit neither aims and scope of this conference, nor the usual length of its papers. One of the questions studied in this paper, namely reflection patterns, does require optimization, but we simply refer to the paper by (Wang et al., 2013) and use optimization as a black box.

We briefly mention further previous work in this area. Controlling patterns created by light is an important topic in various fields, e.g. both Computer Graphics and Architecture. For computational approaches, we refer to (Papas et al., 2011), (Kiser et al., 2012) for modeling caustics, and to (Weyrich et al., 2009) for modeling "microgeometry" reflections. As already mentioned, the main reference for the computational part of the present paper is (Wang et al., 2013). The differential geometry aspects which occur in modeling reflections are treated by (Pottmann and Wallner, 2001), as are the basics of kinematic geometry which we need for stability considerations.

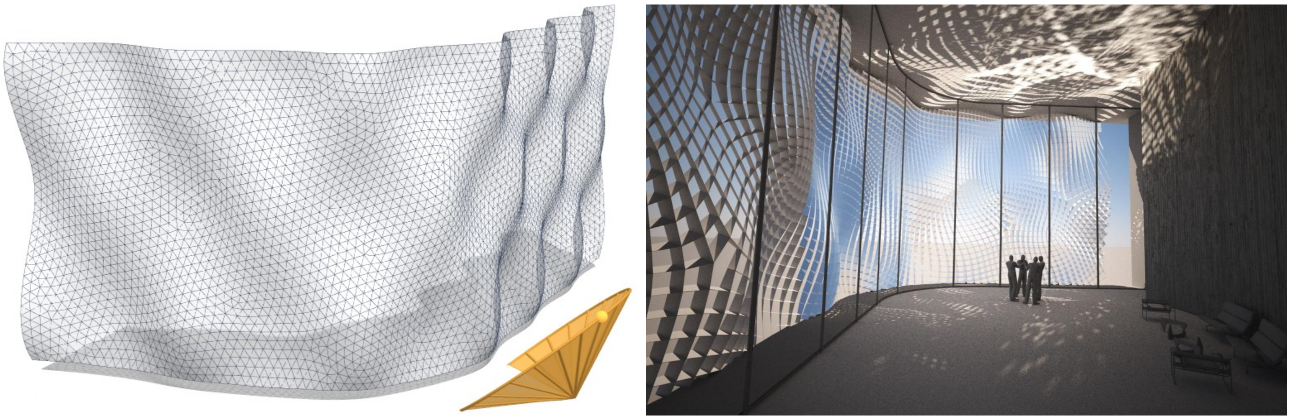

Figure 3: *Left:* Reference surface with sun path. *Right:* Shading system optimized for blocking light for a given sun position, for shallow shading fins, and for reflecting light onto the ceiling. Here the detailed shape of the reflection patterns is not the subject of optimization, only the general direction of outgoing light is. This example is taken from (Wang et al., 2013).

DESIGNING REFLECTION PATTERNS

We here discuss the design of a torsion-free support structure which functions as a system of fins which reflect incoming light towards a given light pattern. Artificial examples of such desired reflection patterns can be seen in Fig. 4. As regards the three-level geometry hierarchy mentioned above, we assume that a reference surface "Φ" is given, and so is a domain "Φ^*", which typically lies in some plane. We wish to determine the 2nd and 3rd geometry layer (base mesh and reflecting fins) such that light hitting Φ is reflected in the fins towards Φ^*.

In the following we describe the modeling procedure in more detail:

- First we find a correspondence which maps points $P \in \Phi$ to points $P^* \in \Phi^*$. For some examples, e.g. if Φ^* is a curve-like domain like the sine wave of Fig. 4c, this is easy: After choosing local coordinate systems for both Φ and Φ^*, this mapping could read $P = (x,y,z) \longmapsto P^* = (ax, b\sin(cy), 0)$, where a,b,c are suitably chosen parameters. For other patterns we use e.g. a correspondence defined by mean value coordinates, cf. (Floater, 2003).
- For each point P we can compute a unit vector L_1 representing incoming light and a unit vector $L_2 = (P^* - P)/\|P^* - P\|$ representing outgoing light. Then the vector $N(P) = L_1 - L_2$ is a normal vector of a plane which can effect the desired reflection (in case we eventually use P as the location of a reflecting fin).
- If a support structure is to effect the desired reflection, then at least one half of the fins must be used for that purpose. The support structures illustrated by Fig. 1 and Fig. 2c generically have four fins adjacent to each node axis, forming a cross. If $P \in \Phi$ marks the location of such a node axis, *two* of these fins must be placed approximately orthogonal to the vector $N(P)$. (Wang et al., 2013) has a method of finding a field of node axes where one half of fins, so to speak, is already determined. We apply that method as a black box, which yields a field of node axes from which a support structure could be derived (that would be the steps depicted in Figs. 2b,c).
- Numerical experiments show that support structures generated by this method do not faithfully reproduce the desired reflection pattern. This is not really to be wondered at since the spatial position of one half of the fins is well-determined by the original correspondence $\Phi \to \Phi^*$ alone, and we cannot expect that a circuitous optimization procedure (known normal vectors of half of the fins $\to$ computing node axes $\to$ computing fins again) yields the very fin distribution we started from.
- Since exactness of fin placement is very important when designing reflection patterns, we reconsider the field of node axes, which is in the stage depicted by Fig. 2a. It comes with a field of suggested "principal" directions, one half of which corresponds to the reflecting fins. We simply apply *correction* to the field of principal directions, replacing the wrong directions with the known directions which stem from the correctly placed fins. From now on the construction of a support structure is the same as applied by (Wang et al., 2013).

We have chosen a sine wave reflection pattern to not only compute, but actually build, a support structure. Fig. 5 illustrates

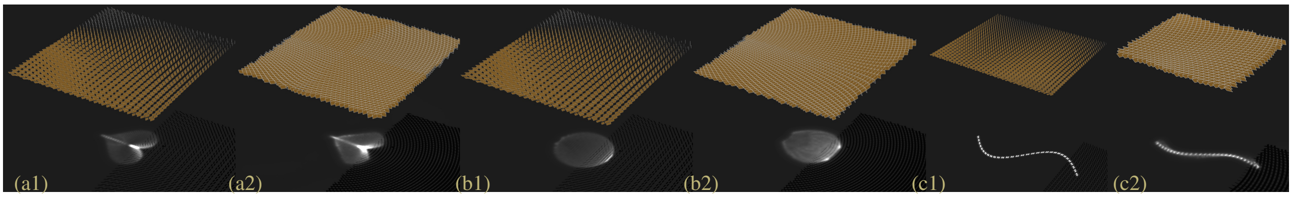

Figure 4: Playing with reflection patterns. The subfigures labelled with “1” show the desired reflection pattern which is to occur if light falls in from a fixed direction and hits an arrangement of fins. The pattern is simulated by rendering the behaviour of planar quads which are uniformly distributed along the reference surface, each of which reflects incoming light towards a certain point in the illuminated region. The subfigures labelled with “2” show the simulated reflection pattern created by a complete arrangement of planar fins which meet their neighbours at node axes.

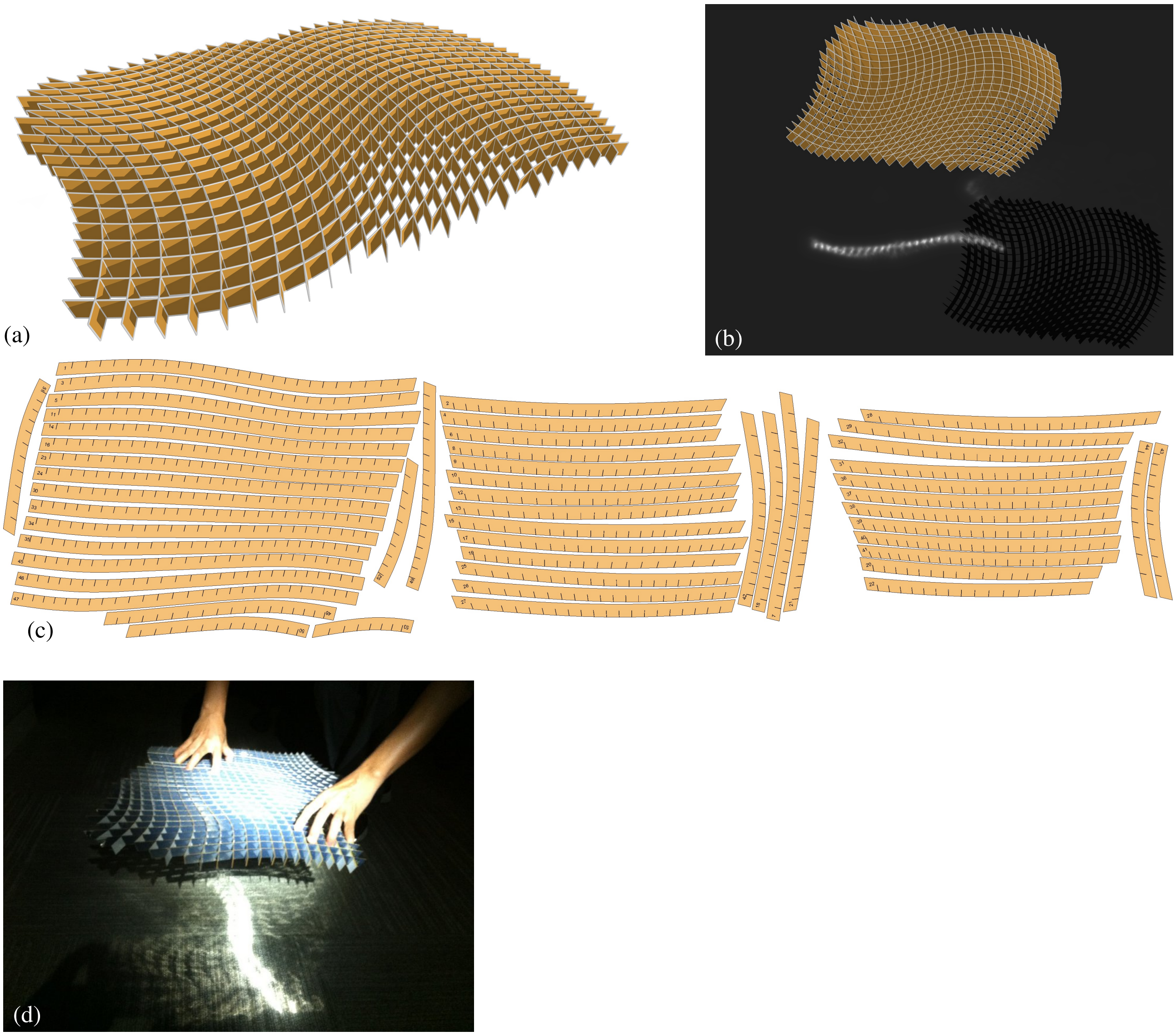

Figure 5: Modeling of reflection patterns. (a) Torsion-free support structure whose fins are to reflect incoming light towards a prescribed shape, in this case a sine wave. (b) simulation of reflection of incoming light in *all* fins, not only that half of fins which is designed to reflect light into the wave. Since the other half of fins does not agree on a common destination for reflected light, the originally intended light distribution is the only one which is clearly visible. (c) shows a cutout pattern for strips which can be bent along node axes and stacked together, thus manufacturing the support structure. (d) shows a photo of the actual light distribution obtained by illuminating the model by a strong flashlight.

the computed support structure, a simulation of light reflected in the support structure, a cutout pattern for manufacturing (anticipating the next section), and a photo of the actually occurring reflections which were created with a flashlight.

Remark. Differential geometers will recognize the node axes as the elements of a line congruence; planar fins approximate torsal planes. The procedure above mimics the differential-geometric fact that one family of torsal planes determines the lines of the congruence and in turn the other family of torsal planes.

MANUFACTURING

Torsion-free support structures have two geometric properties which are relevant for manufacturing, viz., the planarity of fins, and the fact that successive fins meet each other in a node axis. These properties suggest at least two ways of manufacturing.

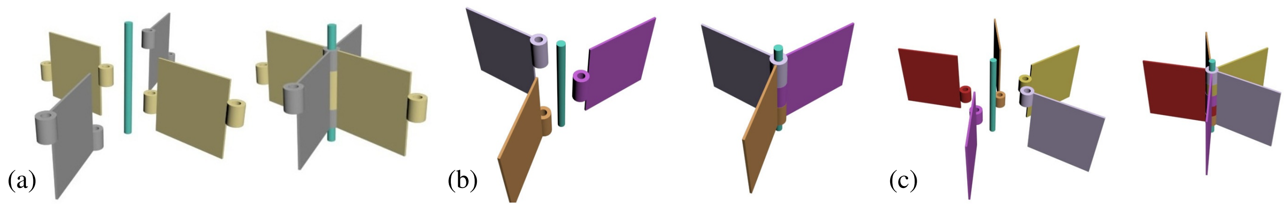

Figure 6: A way of connecting shading fins at node axes. Subfigures (a)–(c) respectively illustrate the regular case of 4 fins joining in the node axis, and the singular cases of 3 and 5 fins.

One of them is shown by Fig. 6. Here shading fins are connected to each node axis in a way which does not transmit moments about that axis. Another one is depicted in Fig. 7 and consists in collecting a sequence of successive fins in a strip which can be developed into the plane. After cutting out these strips and cutting slits into the strips where the node axes are going to be, one can bend the strips into shape and assemble them as shown in Fig. 7.

The second method requires that the material used for manufacturing allows for the necessary bending, while still discharging all structural functions. For applications whose dimensions are close to the glass canopy of Fig. 1 it is unlikely that a manufacturing solution will be anything like cutting out strips and bending them. Obviously for each realization of a support structure in practice the manner of manufacturing must be chosen in a way which minimizes costs, under the side conditions specific to that application. The two properties mentioned above are helpful in any case.

STABILITY

An important question to be asked is if “support structures” are *stable*. We here present an approach to this question which avoids a full-blown finite element analysis and investigation of forces and stresses, but instead investigates the possibility of the structure being *flexible* and, in consequence, unstable. This approach works by assuming that the structure consists of individual rigid bodies which are connected together by hinges. Those rigid bodies could be the individual shading fins of a support structure which are connected according to Fig. 6; or they could be rigid developable strips consisting of successive fins like the ones shown in Fig. 7, with “hinge” connections at each node axis. In the following we describe in more detail an algorithm to determine the degree of flexibility or rigidity of any such system consisting of rigid bodies connected with hinges.

Algorithm. We enumerate all rigid bodies and call them $\Sigma^1, \ldots, \Sigma^N$. If Σ^i and Σ^j are connected by a hinge, we choose two points A^{ij}, B^{ij} on the hinge and declare them to belong to both Σ^i and Σ^j. It is well known that for any rigid body motion of the system Σ^i the velocity state of Σ^i is governed by the vector C^i of angular velocity, and another vector $\bar{C}^i$ which is the velocity experienced by the origin of the coordinate system; the velocity experienced by any point P connected to Σ^i is then given by

$$V^i(P) = C^i \times P + \bar{C}^i, \qquad (*)$$

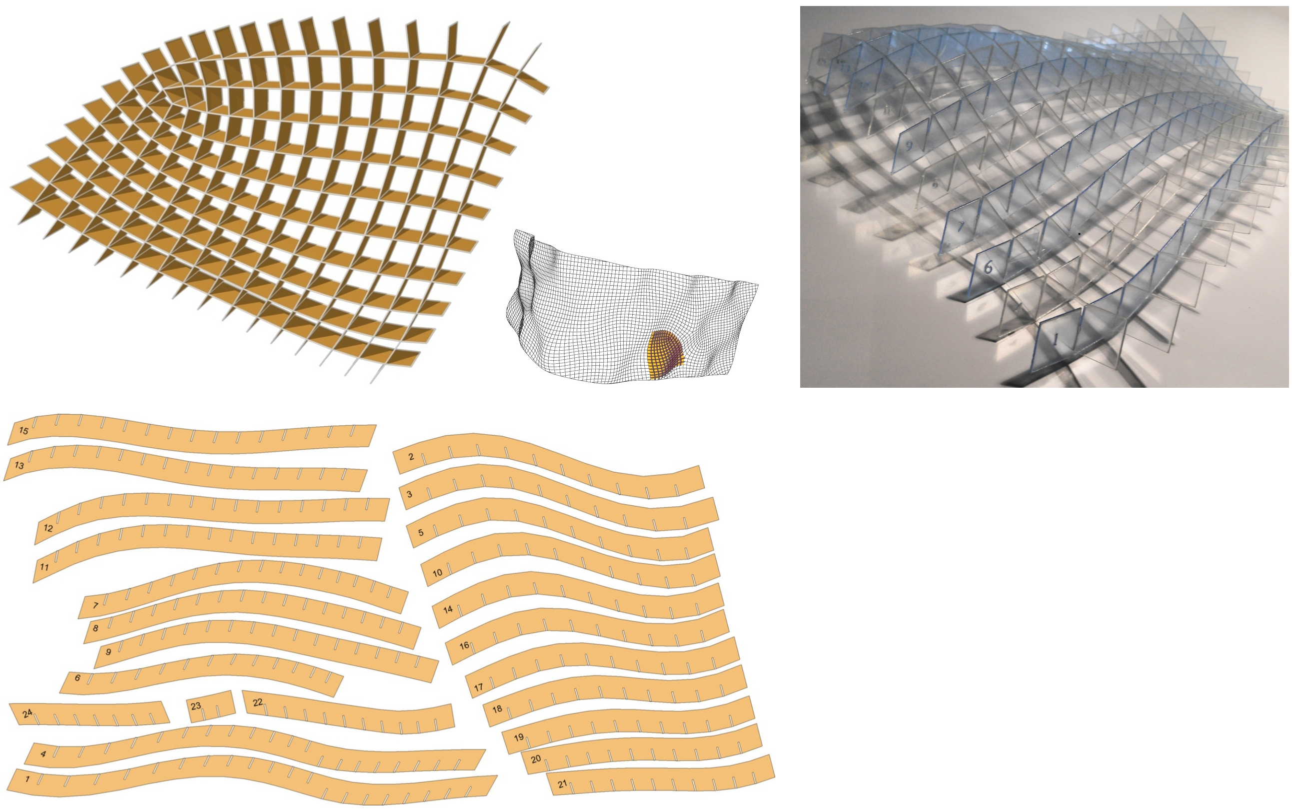

Figure 7: Building a model. This arrangement of strips is part of the larger shading and lighting system shown by Fig. 3. Strips consisting of successive shading fins have been developed into the plane, cut out from acrylic glass, and stacked together. *Left:* Cutout pattern of strips. *Top:* Rendering of shading system and photo of the acrylic glass model.

cf. (Pottmann and Wallner, 2001). Bodies which are connected cannot move independently; for each hinge we have the conditions

$$C^i \times A^{ij} + \bar{C}^i = C^j \times A^{ij} + \bar{C}^j, \quad C^i \times B^{ij} + \bar{C}^i = C^j \times B^{ij} + \bar{C}^j, \tag{**}$$

which express the fact that the points A^{ij} and B^{ij} on the hinge must experience the same velocity, regardless of the system they belong to.

Since the entire arrangement of rigid bodies can always move as a single rigid body, the linear system (**) has a 6-dimensional space of "trivial" solutions. In order to eliminate these we constrain one system, to remain at rest. Assuming our arrangement of systems and hinges is still flexible, there will be a nonzero velocity state which solves Equation (**); otherwise the only solution will be zero velocities. In order to determine how far our arrangement is from being flexible, we solve for a best-possible solution of (**) under the side condition that each system *must* move. It is well known that the solution is obtained by the following standard procedure:

1. We constrain one system, say Σ^1, to remain at rest by enforcing $C^1 = (0,0,0)$ and $\bar{C}^1 = (0,0,0)$. There remain $2(N-1)$ unknown vectors $C^2, \bar{C}^2, \ldots, C^N, \bar{C}^N$.
2. The system (**) represents two vector equations per hinge, and a total of 6 scalar equations per hinge. If the number of hinges is denoted by H, we get a total of $6H$ scalar equations for the $6N$ scalar components c_1^i, c_2^i, c_3^i, $\bar{c}_1^i$, $\bar{c}_2^i$, $\bar{c}_3^i$ $(i = 1, \ldots, N)$ of which $6(N-1)$ are unknown. Actually these 6 scalar equations per hinge only count as 5 equations, because they are linearly dependent, but this detail is not essential here.
3. We put the $6(N-1)$ variables $c_1^2, c_2^2, c_3^2, \ldots, \bar{c}_1^N, \bar{c}_2^N, \bar{c}_3^N$ in a single column vector X, and write the the linear conditions (**) in the form $AX = 0$ with a certain matrix A of $6H$ rows and $6(N-1)$ columns.
4. The above-mentioned best possible solution is more precisely defined as the minimizer of $\|AX\|$ under the condition $\|X\| = 1$, where the usual 2-norm for vectors is employed.

5. It is well known that the solution X is given as the first row of the matrix V in a singular value decomposition $A = UDV$, where U, V are orthogonal matrices and D is a rectangular-diagonal matrix whose nonnegative diagonal entries are sorted in ascending order.

The resulting vector X represents velocity states of the individual rigid bodies which are *as consistent as possible* in the sense that the deviation of velocities in the hinges is minimal (in the least squares sense). In case this mechanism is truly flexible, the deviation of velocities will vanish, and (**) will be fulfilled exactly for all hinges.

Interpretation of Results. The computations described in the previous paragraph yield a velocity state $(C^i, \bar{C}^i)$ for each rigid component of a support structure. In particular, each point "P" belonging to system Σ^i is assigned a velocity $V^i(P) = C^i \times P + \bar{C}^i$. We now let each point move for a time interval of 1 second, so that P moves to the new position $P + V^i(P)$. For a hinge point we may compute the updated positions w.r.t. both systems it belongs to. The discrepancy

$$\big(P + V^i(P)\big) - \big(P + V^j(P)\big) = V^i(P) - V^j(P)$$

experienced by that hinge is illustrated by Fig. 8. One can clearly see that in case the entire strips are considered rigid, the deviation at hinges is way too high to be accommodated by the usual leeway present in connections; whereas in case each individual fin is rigid, this deviation is rather small, so that for all practical purposes the arrangement must be considered flexible — in consequence, the fin arrangement of Fig. 7, connected via hinges as shown by Fig. 6, is unstable and cannot be expected to bear loads (including the dead load) unless the connection is made rigid so as to transmit moments also.

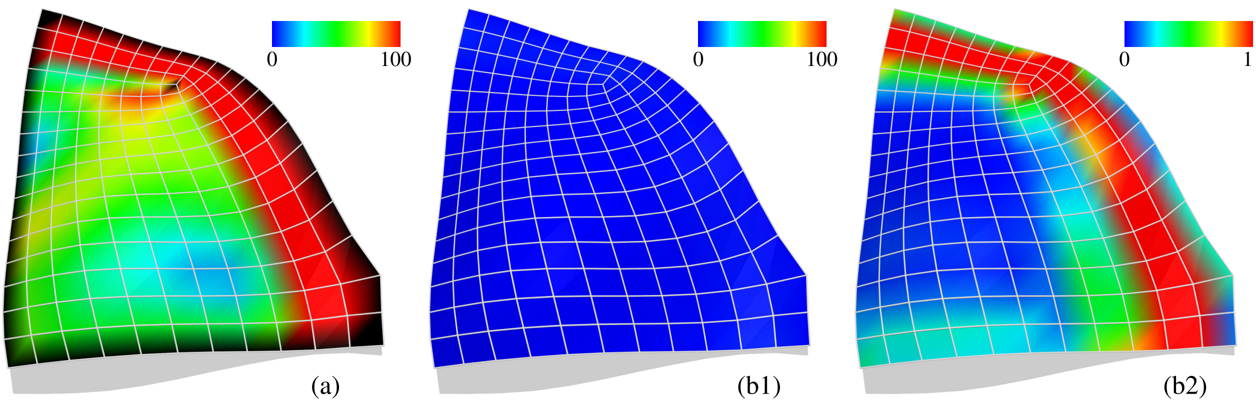

(a) (b1) (b2)

Figure 8: Illustration of stability of a shading system via its rigidity. In (a) the long strips of Fig. 7 are considered rigid, while in (b1) and (b2) each shading fin is a rigid body of its own. In all cases the node axes act as hinges. The object is scaled such that the average distance of nodes from the barycenter is 1000 units of length. The velocities of an almost consistent flexion are computed as described in the text; velocities are normalized by fixing one system and letting the velocity of a distance node equal $1\,unit/sec$. The colors illustrate the discrepancy experienced by hinge vertices after traveling for $1\,sec$.

CONCLUSION

After reporting on motivation we reviewed the capabilities of a computational approach to shading and lighting systems published by (Wang et al., 2013). This paper extends the applications given there, in particular we given examples where reflection patterns are designed. A main focus of this paper is manufacturing: We not only demonstrate cutout patterns corresponding to shading and lighting systems, but we also study the stability of such systems. The methods which are employed in this analysis are kinematic in nature and are founded on the principle that flexibility and stability exclude each other. In conclusion we believe that this topic of controlling light and shade is an attractive one which involves different disciplines, in particular geometry processing, and which can benefit from each other.

REFERENCES

Floater, M. S., 2003. Mean value coordinates. *Comp. Aided Geom. Design*, 20:19–27.

Kiser T.; Eigensatz M.; Nguyen M. M.; Bompas P.; Pauly M., 2012. Architectural caustics – controlling light with geometry. In L. Hesselgren et al., editors, *Advances in Architectural Geometry 2012*, pages 91–106. Springer.

Papas M.; Jarosz W.; Jakob W.; Rusinkiewicz S.; Matusik W.; Weyrich T., 2011. Goal-based caustics. *Computer Graphics Forum*, 30(2):503–511, Proc. Eurographics.

Papas M.; Houit T.; Nowrouzezahrai D.; Gross M.; Jarosz W., 2012. The magic lens: refractive steganography. *ACM Trans. Graph.*, 31(6):186:1–186:10, Proc. SIGGRAPH Asia.

Pottmann H.; Wallner J., 2001. *Computational Line Geometry*. Springer.

Wang J.; Jiang C.; Bompas P.; Wallner J.; Pottmann H., 2013. Discrete line congruences for shading and lighting. *Computer Graphics Forum*, 32(5):53–62, Proc. Symposium Geometry Processing.

Weyrich T.; Peers P.; Matusik W.; Rusinkiewicz S., 2009. Fabricating microgeometry for custom surface reflectance. *ACM Trans. Graph.*, 28(3):32:1–32:6, Proc. SIGGRAPH.